

Single Polymer Chain Elongation by Atomic Force Microscopy

Jason E. Bemis, Boris B. Akhremitchev, and Gilbert C. Walker*[†]

Department of Chemistry, University of Pittsburgh, Pittsburgh, Pennsylvania 15260

Received July 10, 1998. In Final Form: February 3, 1999

The elastic deformation of single polystyrene-*b*-poly-2-vinylpyridine chains from spun cast films was investigated by atomic force microscopy. A nonlinear elastic response is shown to be present hundreds of nanometers above the bulk surface. The length of the elastic response monotonically increases with molecular weight of the polymer. These nonlinear elastic responses are fit to wormlike chain and freely joined chain models giving persistence and Kuhn lengths of approximately 3 and 4 Å, respectively. The entropic models reveal that the polymer chains are stretched to 80–90% of their contour length before the attachment to the tip is ruptured.

Introduction

The understanding of adhesive properties of two surfaces in contact requires the detailed comprehension of the molecular interactions between the surfaces. This is necessary in numerous applications, from the agglutination of two surfaces, to the preparation of anti-fouling surfaces. Previous atomic force microscopy (AFM) studies of adhesion have focused on the intersurface properties from both experimental and theoretical standpoints.^{1–6} Recent developments in AFM have allowed for the manipulation of single polymer chains,^{7–11} providing an unprecedented opportunity to test molecular theories of adhesion. We are examining molecular adhesion, by investigating the interaction of a single commercial polymer chain between the tip of an AFM and the surface.

Figure 1 shows a schematic representation of polymer attachment to an AFM tip. If one or more chains are attached to the tip after the tip jumps free of the surface, the tip will experience an adhesive force away from the surface until it breaks free from the polymer chains. Entropic spring models of polymer chains have been used to explain polymer stretching.^{10–12} The principal models considered here are the freely joined chain (FJC) and the wormlike chain (WLC). The FJC model predicts force–distance behavior described by the inverse Langevin

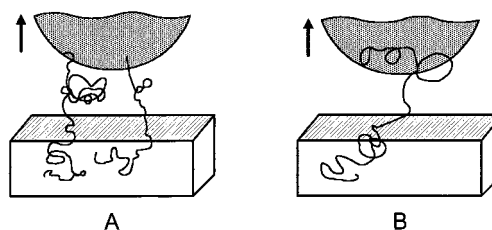


Figure 1. (A) Multichain model. When multiple elastic responses are observed, as in Figure 3, this model accounts for each response as a separate chain. This implies that the entire elastic response of each chain is observed and that the force plot must be deconvoluted to determine the persistence or Kuhn length of each individual chain (as shown in Figure 3a). (B) Single chain model. Multiple elastic responses can also be explained by multiple attachments of a single chain from the tip and/or surface. This can result from multiple attachments on the tip/surface, where each rupture increases the fraction of the chain being stretched. The single chain model includes independent elastic responses, which results in lower and more consistent fitted persistence and Kuhn lengths, when compared to the multichain model.

function $\mathcal{L}^*(R) = \beta$, where the Langevin function, $\mathcal{L}(R) = \coth(\beta) - 1/\beta$, as shown by eq 1.¹³

$$F = (kT/A_k) \mathcal{L}^*(R) \quad (1)$$

Here F is the tension between two points (nN), k and T are the Boltzmann constant (aJ/K) and temperature (K), respectively, A_k is the Kuhn length (nm), and R is the unitless extension ratio. The extension ratio is the fraction of the polymer contour length that the chain is extended. If points A and B are separated by distance x , the extension ratio is x over the contour length of the chain between points A and B. The WLC model predicts a force–distance dependence described by eq 2.

$$F = (kT/q) (0.25(1 - R)^{-2} - 0.25 + R) \quad (2)$$

where q is the persistence length (nm).

In this article, we report our examination of polystyrene-*b*-poly-2-vinylpyridine, which has been of widespread interest.^{14–20} The hydrophobic–hydrophilic block dynam-

* To whom correspondence should be addressed.

[†] 3M Untenured Faculty Awardee.

(1) Aime, J. P.; Elkaakour, Z.; Odin, C.; Bouhacina, T.; Michel, D.; Curely, J.; Dautant, A. *J. Appl. Phys.* **1994**, *76*, 754–762.

(2) Burnham, N. A.; Colton, R. J.; Pollock, H. M. *Nanotechnology* **1993**, *4*, 64–80.

(3) Hoh, J. H.; Cleveland, J. P.; Prater, C. B.; Revel, J. P.; Hansma, P. K. *J. Am. Chem. Soc.* **1992**, *114*, 4917–4918.

(4) Magonov, S. N.; Reneker, D. H. *Annu. Rev. Mater. Sci.* **1997**, *27*, 175–222.

(5) Sasaki, M.; Hane, K.; Okuma, S.; Bessho, Y. *Rev. Sci. Instrum.* **1994**, *65*, 1930–1934.

(6) Zhulina, E. B.; Walker G. C.; Balazs, A. C. *Langmuir* **1998**, *14*, 4615–4622.

(7) Chatellier, X.; Senden, T. J.; Joanny, J. F.; DiMaggio, J. M. *Europhys. Lett.* **1998**, *41*, 303–308.

(8) Florin, E. L.; Moy, V. T.; Gaub, H. E. *Science* **1994**, *264*, 415–417.

(9) (a) Noy, A.; Vezenov, D. V.; Kayyem, J. F.; Meade, T. J.; Lieber, C. M. *Chem. Biol.* **1997**, *4*, 519–527. (b) Lee, G.; Chrisey, L.; Colton, R. *Science* **1994**, *266*, 771–773.

(10) Rief, M.; Gautel, M.; Oesterhelt, F.; Fernandez, J. M.; Gaub, H. E. *Science* **1997**, *276*, 1109–1112.

(11) Rief, M.; Oesterhelt, F.; Heymann, B.; Gaub, H. E. *Science* **1997**, *275*, 1295–1297.

(12) Marko, J. F.; Siggia, E. D. *Macromolecules* **1995**, *28*, 8759–8770.

(13) Flory, P. J. *Statistical Mechanics of Chain Molecules*; Interscience: New York, 1969.

(14) Koneripalli, N.; Levicky, R.; Bates, F. S.; Ankner, J.; Kaiser, H.; Satija, S. K. *Langmuir* **1996**, *12*, 6681–6690.

Table 1. Summary of Strand Elongation Length and Force^a

polymer	length of blocks (nm) [total length]	mean length of elastic response (nm)	maximum length of elastic response (nm)	median rupture force of elastic response (pN)	elastic event probability	relative trigger (nm)	z scan size (nm)	z scan rate (Hz)
PS7800–P2VP10000	19/24 [43]	24.5	59.3	170 ± 40	0.30	50	130	4.88
PS13800–P2VP47000	33/112 [145]	42.0	92.6	210 ± 30	0.03 ^c	30	300	5.58
PS52400–P2VP28100	126/67 [193]	44.5	94.1 ^b	150 ± 25	0.52	100	300	1.95
PS60100–P2VP46900	145/112 [257]	68.1	268.8	90 ± 14	0.24	100	500	1.95
PS29100	70	53.5	111.1	280 ± 30	0.22	100	300	4.88
P2VP50000	119	65.2	125.6	120 ± 20	0.44	100	500	9.77

^a The elastic event probability is taken as the number of force plots exhibiting at least one elastic response divided by the total number of plots examined. The trigger is the maximum deflection exerted on the surface. Multiplying the trigger by the spring constant gives the maximum force exerted on the surface. The spring constants were approximately 0.07 ± 0.01 N/m except for the cantilever used on P2VP, which was 0.03 N/m. ^b Force plots shown in Figure 6 were excluded from the maximum. ^c The dependence of the elastic response on contact time is provided in Table 3 (supporting information).

ics offer a wide range of applications, such as an interfacial bridge between immiscible homopolymers.¹⁹ Models of adhesion between two surfaces in contact, such as JKR, are well developed but fail to describe the appreciable adhesion when the surfaces are bridged by polymer chains.

Experimental Section

PS7800–P2VP10000, PS13800–P2VP47000, PS52400–P2VP28100, PS60100–P2VP46900, and P2VP50000 were purchased from Polymer Source (Dorval, Canada); these polymers had polydispersity indices less than 1.11 and were used without further purification. PS29100 was purchased from Aldrich with a polydispersity index of 1.04. Blocks are designated by PS for polystyrene and P2VP for poly-2-vinylpyridine. Molecular weights of the individual blocks are given after the designation for the block in units of daltons. Block copolymers and polystyrene were dissolved in toluene (J. T. Baker) that was filtered with a 0.45 μm nylon membrane. P2VP was dissolved in THF (EM Science); all solutions were approximately 2 g/L.²¹ Samples were prepared by spin casting onto 12 mm diameter glass cover slips (Fischer Scientific) at 1000 rpm for 2 min using a Headway Research ED101D photo resist spinner.

All AFM measurements were conducted using a Digital Instruments (Santa Barbara, CA) Nanoscope IIIa Multimode scanning force microscope, typically in force volume mode. The spring constants were calibrated using a Park Scientific Instruments force constant calibration cantilever (Sunnyvale, CA), according to eq 3.²³

$$K = K_{\text{ref}}(\text{sensitivity} - \delta_{\text{test}})/(\delta_{\text{test}} \cos \theta) \quad (3)$$

δ_{test} is the sensitivity (V/nm) on the reference standard, $K_{\text{ref}} = 0.157$ N/M, and θ is the angle of the cantilever with respect to the surface, taken as 11° . Tip shapes were characterized by scanning a grating of 700 nm high, 20° cone angle, 10 nm radius tips (NT-MDT Moscow, Russia) to ensure minimal contamination of the tip. Tip radii were found to be on the order of 50–100 nm. All measurements were done in 0.45 μm filtered 10 mmol sodium acetate buffer using a Digital Instruments fluid cell. Sodium acetate was purchased from EM Science. Water was purified using a Barnstead NANO pure filter to 18 M Ω resistivity.

Force volumes of $16 \times 16 \times 512$ points were collected using Nanoscope IIIa software and analyzed using custom software written for Matlab (Math Works, Inc., Natick MA). Persistence lengths and maximum extension ratios were obtained by fitting the elastic response curves to the WLC model and minimizing χ^2 . All χ^2 values are reduced χ^2 , with the uncertainty determined from the tail of the retrace data. Kuhn length and maximum extension ratios were obtained by fitting the elastic response

curves to an approximation²⁴ of the FJC model, as there is no exact solution of the inverse Langevin function, and minimizing χ^2 . Relevant experimental scanning parameters are given in Table 1.

Contact angle measurements were conducted using a home-built apparatus. The sample was housed in an environmental chamber that was continually flushed with humidified nitrogen. Images were collected using a CCD camera and video capture software. A Zisman plot of P2VP50000 was constructed from a series of aqueous NaCl solutions 0, 5.43, 10.46, 14.92, 22.62, and 25.92% (w/w) (Supporting Information).

Results and Discussion

The surface topography of the block copolymers was typically irregular with sporadic height features on the order of 100 nm. There were ample areas ($\sim 1 \mu\text{m}^2$) that were devoid of height features greater than 15 nm. All force volume measurements were conducted in such areas so as to remove height aberrations from the force plots. There were small (~ 50 nm wide, 5 nm high) ordered structures, which may have possibly been micellular in nature.¹⁸ These features were not observed in air, although this may have been due to the higher scanning forces

(15) Meiners, J. C.; Ritz, A.; Rafailovich, M. H.; Sokolov, J.; Mlynek, J.; Krausch, G. *Appl. Phys. A* **1995**, *61*, 519–524.

(16) Parsonage, E.; Tirrell, M.; Watanabe, H.; Nuzzo, R. G. *Macromolecules* **1991**, *24*, 1987–1995.

(17) Pelletier, E.; Stamouli, A.; Belder, G. F.; Hadziioannou, G. *Langmuir* **1997**, *13*, 1884–1886.

(18) Stamouli, A.; Pelletier, E.; Koutsos, V.; Vegte, E. V. D.; Hadziioannou, G. *Langmuir* **1996**, *12*, 3221–3224.

(19) Shull, K. R.; Kramer, E. J.; Hadziioannou, G.; Tang, W. *Macromolecules* **1990**, *23*, 4780–4787.

(20) Tang, W. T. Ph.D. Thesis, Stanford University, 1987.

(21) Static light scattering reveals that the critical micelle concentration (cmc) of PS–P2VP solutions in toluene is approximately 65 $\mu\text{g}/\text{mL}$,²⁰ and as such, much of the work with PS–P2VP has been above the cmc. Adsorption of polystyrene-poly(ethylene oxide) block copolymers from selective solvents above the cmc provide inhomogeneous film thickness and surface coverages.²² However, the surface morphology of films made from toluene solutions of PS–P2VP block copolymers in the concentration range of 0.1–6 mg/mL are surprisingly uniform.¹⁷ Part of the reason that the films are so homogeneous, even when the film is made from a solution above the cmc, is that there is an appreciable concentration of unimers above the cmc.²⁰ Above 6 mg/mL there is a series of “wormlike” ridges.¹⁷ By use of solutions below this second critical concentration, this morphology is avoided, simplifying the force–distance analysis.

(22) Munch, M. R.; Gast, A. P. *Macromolecules* **1990**, *23*, 2313–2320.

(23) Tortonesi, M.; Kirk, M. *Micromach. Imaging* **1997**, *3009*, 53–60.

(24) $\Delta^*(R) = \pi/2R^6 \tan(R\pi/2) + (1 - R^6) P(R) = \beta$. Here R is the extension ratio of the polymer, and $P(R)$ is a 19th order polynomial, whose coefficients in decreasing order are 1.76×10^8 , -1.48×10^9 , 5.74×10^9 , -1.36×10^{10} , 2.18×10^{10} , -2.53×10^{10} , 2.19×10^{10} , -1.44×10^{10} , 7.24×10^9 , -2.79×10^9 , 8.22×10^8 , -1.83×10^8 , 3.01×10^7 , -3.59×10^6 , 2.97×10^5 , -1.61×10^4 , 5.24×10^2 , -8.73 , 3.06 , -6.36×10^{-5} . The polynomial was obtained by fitting the inverse Langevin function to the above expression and has a mean relative error of 0.0035 in the range of $R = 0.001$ to 0.999. It should be noted that the expansion series found in previous works¹³ fail to fit higher extension ratios (> 0.85).

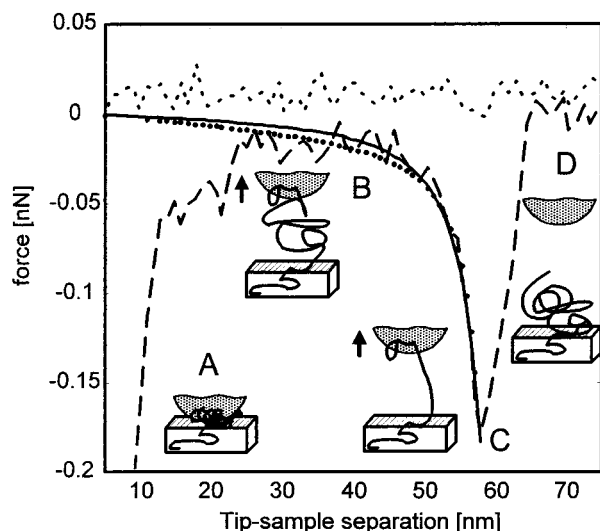


Figure 2. PS60800–P2VP46900 collected with a 100 nm trigger, 500 nm *z* scan size, and 1.95 Hz *z* scan rate. The upper dotted line is the advancing tip and the dashed line is the withdrawing tip. The solid line is a wormlike chain (WLC) fit to the elastic response observed after the tip jumped off the surface. The persistence length is 5.75 Å, maximum extension ratio 0.90, and χ^2 of 1.52. The lower dotted line is a freely joined chain (FJC) fit to the same response with a Kuhn length of 5.86 Å, maximum extension ratio of 0.96, and χ^2 of 1.45. (A) The tip jumps free of the surface. (B) The tip elastically deforms a polymer chain still attached to the tip. (C) The tip jumps free of the polymer chain; we often referred to this as the rupture point. (D) The tip remains at zero deflection for the remainder of the scan.

induced by capillary forces. The topography of the homopolymer was similar to the block copolymer, with the absence of the aforementioned structures. All samples were scanned in sodium acetate to decrease the force of adhesion by means of the double layer formed around the silicon nitride tip. This decrease in force of adhesion (from 1.7 to 1.1 nN) decreases the distance the tip travels when it jumps free of the surface, in turn increasing the distance over which data are obtainable.

Figure 2 represents a typical force plot in which an elastic response is observed. At point A in the retracting plot, the tip jumps free from the surface. It slowly goes to zero deflection until point B, 45 nm above the surface, where the tip begins to experience significant elastic tension from the attached polymer chain. At point C, 58 nm from the surface, the chain breaks free from the tip. This point is taken as the point of rupture, giving the length and force of the elastic response, 58 nm and 180 pN in this case. After this point, the tip returns to zero deflection (point D) for the remainder of the *z* travel (360 nm). The elastic response of the polymer is calculated from points A to C, although the error function used in the fitting only included the region from B to C.

Table 1 summarizes the statistical analysis of data collected. The lengths of the blocks were estimated from the covalent radii of carbon (0.77 Å), the C–C bond angle of 109.5°, and the number of monomers for the chain. The data represented in Table 1 are comprised of different types of elastic responses. The single elastic response shown in Figure 2 is the response most frequently observed. Occasionally, multiple elastic events were observed in a single force plot, as shown in Figure 3, which represent a smaller, but appreciable, content of the data.

The elastic response of the polymer samples can be fit by both FJC and WLC models, as shown by Figure 2, the FJC being the dotted line. The statistical analysis of fitted

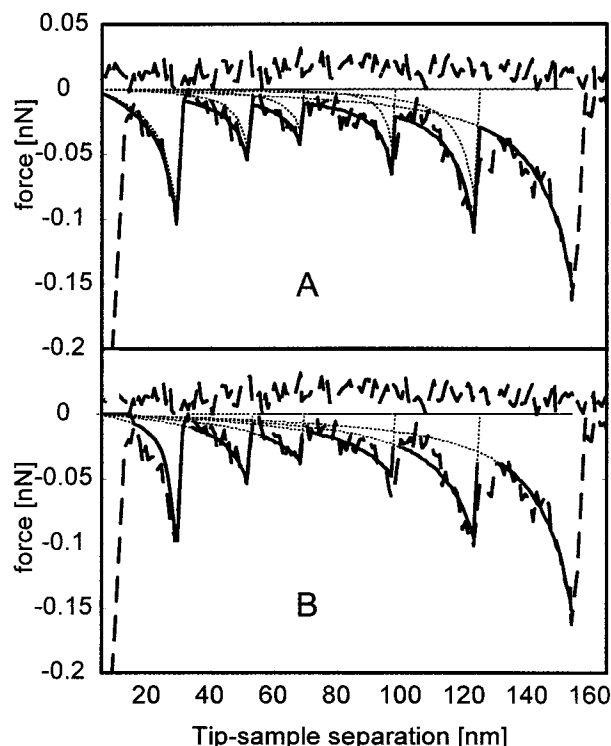


Figure 3. PS60800–P2VP46900 collected with a 100 nm trigger, 500 nm *z* scan size, and 1.95 Hz *z* scan rate. (A) The multichain, multipersistence length WLC fit is shown as the solid line with the individual chain responses shown as the thin dashed lines. From left to right, the persistence lengths and maximum extension ratios are 1.9 Å and 0.75, 12.0 Å and 0.86, 22.0 Å and 0.88, 63.0 Å and 0.94, 21.0 Å and 0.92, and 4.7 Å and 0.88. The fit gave a χ^2 of 1.09. (B) Single chain fit with a single persistence length of 4.4 Å and χ^2 of 1.96. From left to right, the maximum extension ratios are 0.86, 0.78, 0.73, 0.77, 0.84, and 0.87. The solid line is the sum of the dotted thin lines.

values obtained from both models is summarized in Table 2. When the maximum extension ratio is a free parameter, the major difference in the fits to the two models is found in the low force, low extension ratio regime (from 25 to 45 nm tip–sample separation in Figure 2). The noise in the data (10–20 pN standard deviation) at this low force and the quality of the resulting fits to the two models preclude the choice of one model over the other, as demonstrated by χ^2 values. This is not entirely surprising as the WLC model requires only a small persistence length to fit the data well. The noise also results in shallow error functions for the persistence and Kuhn lengths.

We now examine the supposition that the majority of the elastic responses correspond to probing a single polymer chain. It is possible to estimate the number of chains between the tip and the surface based on the length and diameter. The diameter of the chain can be estimated from the Young modulus of the bulk and the persistence length.

$$D = (32qkT/(\pi E))^{1/4} \quad (4)$$

Here *D* is the chain diameter and *E* is the Young modulus (3 GPa for polystyrene). Figure 4 shows the persistence length and corresponding diameters for the multichain WLC fits. Kuhn lengths, and corresponding diameters can be found in Supporting Information. The fourth root of the persistence length in eq 4 compensates for the large uncertainty of this parameter, so that the diameter of the chains has been accurately determined to be 2.5 ± 0.5 Å. This molecular scale diameter strongly suggests that a

Table 2. Fitted Parameters for the Wormlike Chain and Freely Joined Chain Models^a

polymer	WLC			FJC		
	median persistence length (Å)	mean maximum extension ratio	mean χ^2	median Kuhn length (Å)	mean maximum extension ratio	mean χ^2
PS7800–P2VP10000	3.0 ± 2.6	0.85 ± 0.04	2.5 ± 1.1	3.6 ± 2.7	0.94 ± 0.02	2.7 ± 1.4
PS13800–P2VP47000	2.4 ± 2.1	0.85 ± 0.11	1.3 ± 1.2	3.0 ± 4.0	0.91 ± 0.08	1.6 ± 1.5
PS52400–P2VP28100	2.9 ± 11.3	0.84 ± 0.08	1.5 ± 0.7	4.0 ± 11.6	0.94 ± 0.03	1.6 ± 0.7
PS60100–P2VP46900	4.5 ± 14.0	0.83 ± 0.10	1.9 ± 0.9	5.8 ± 10.5	0.88 ± 0.18	1.8 ± 0.9
PS29100	3.7 ± 21.1	0.90 ± 0.05	3.3 ± 3.9	3.7 ± 6.4	0.96 ± 0.02	3.4 ± 3.6
P2VP50000	4.0 ± 3.2	0.81 ± 0.07	1.5 ± 0.4	5.8 ± 2.8	0.91 ± 0.05	1.9 ± 0.6
all polymers	2.9 ± 10.5	0.82 ± 0.21	1.7 ± 1.7	3.8 ± 7.1	0.92 ± 0.09	1.9 ± 1.8

^a The maximum extension ratio is the ratio of the entire length of the chain between the tip and the surface divided by the distance at which the chain ruptures. \pm Values are standard deviations. "All polymers" represents all molecular weights of block copolymer and homopolymer studied.

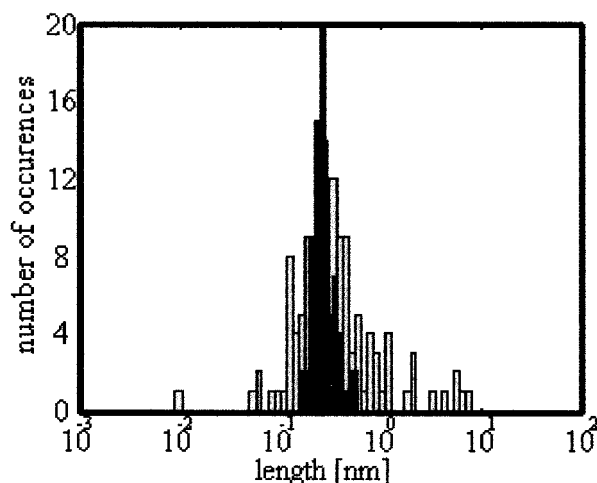


Figure 4. The gray histogram represents the persistence lengths obtained from multichain WLC fits to elastic responses. This histogram is the sum of all polymers studied as there is no noticeable difference in persistence lengths between molecular weights of block copolymers or homopolymers (see Table 2). The black histogram is the corresponding diameters to the persistence lengths.

single chain is being extended, or that the chains are being stretched in series.

An analysis of the length of the elastic response shows that it is unlikely that chains extended in series. Figure 5 shows the length of the elastic response plotted versus length of chain (solid line connecting data), which may be fit by a straight line. We conjecture that the slope obtained from the fit (0.2) is a consequence of chain entanglement. Longer chains are more likely to be entangled, and the length to which they may be extended is proportionally smaller than the full length.²⁵ The estimated contour length of the chain between the tip and the surface based on the extension ratio obtained from the WLC fits is plotted as a function of chain length in Figure 5 (dashed line). The estimated contour length is calculated by dividing the length of the elastic response by the maximum extension ratio. The extension ratios obtained with the FJC are higher, and so the estimated contour length of the chains based on that model will lie between the two lines shown. This estimated contour length of the chains is significantly less than the molecular-weight-based estimate of the length of chains (Table 1). This discredits the interpretation that chains are being extended in series, in turn reinforcing our conclusion that most of the time a single chain is being stretched. The maximum length of the elastic response given in Table 1 shows that

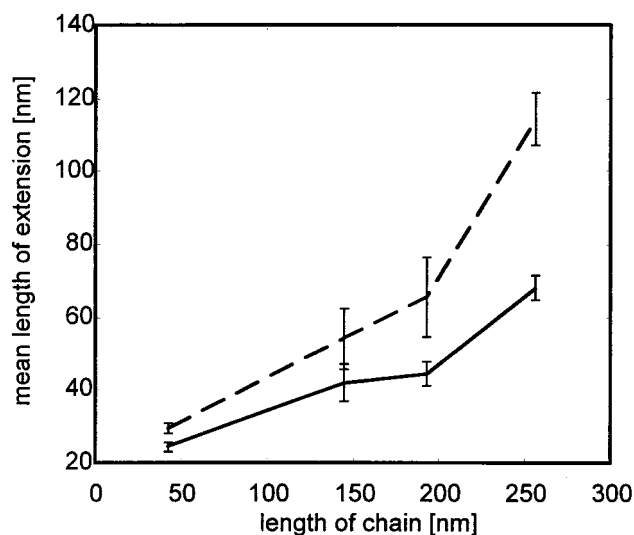


Figure 5. Four molecular weights of PS–P2VP (see Table 1). The x axis is the polymer chain length, where the values are estimated from the molecular weights as described in the text. The lower solid line is the mean tip–sample separation at the rupture of the elastic response. The upper dashed line is the contour length of the chain between the tip and surface estimated from the maximum extension ratios obtained from the WLC model fits.

occasionally (~3%) there is an elastic response that exceeds the estimated length of the chains. This can be accounted for by the small amount of polydispersity.

We have also considered volume exclusion effects. In poor solvent conditions and low tension, a polymer chain will collapse upon itself, forming a series of Pincus blobs.²⁶ This is particularly important at low extensions and has a predicted force–distance dependence as described by eq 5.²⁷

$$F \approx \gamma V^{1/2} D^{-1/2} \quad (5)$$

Here γ is the interfacial tension, V is the volume of the polymer globule that remains on the surface, and D is the distance the chain has been pulled out of the globule. This behavior is apparent in Figure 2 from 15 to 25 nm tip sample separation. Our experiments were not optimized to collect data in this region of the force curve, but fits using eq 5 are reasonable. As this is the region in which volume exclusion effects are prevalent, we have ignored volume exclusion effects at higher extensions; regions of low tip sample separation and decreasing force with distance were not included in the fits to the elastic models.

(25) Wang, Y.; Winnik, M. A. *J. Phys. Chem.* **1993**, *97*, 2507–2515 and references therein.

(26) Pincus, P. *Macromolecules* **1976**, *3*, 386–388.
(27) Halperin, A.; Zhulina, E. B. *Europhys. Lett.* **1991**, *15*, 417–421.
Halperin, A.; Zhulina, E. B. *Macromolecules* **1991**, *24*, 5393–5397.

Figure 3 shows multiple elastic responses in a single force plot. We consider two fundamentally different ways of explaining the origin of multiple elastic responses: from multiple chains or from multiple attachments of a single chain, as is schematically represented in Figure 1. For the case depicted in Figure 1a, there are two chains attached to the tip. Despite the low polydispersity of the samples, few chains will have identical contour lengths between the tip and surface. Neither the length of the chain on the surface that is free from entanglement nor the position of the tip attachment to the chain are required to be the same for each chain. The observed elastic response will contain contribution from the elastic deformation of both the long and short chains.

In the case of a single chain with multiple attachments to the tip, the rupture of the first attachment exposes a greater contour length of the chain to stretching. In contrast to the multichain model, the rupture of this first attachment is independent of the elastic deformation of the second attachment.

The data in Figure 3a were fit using the multichain model, and the individual elastic responses are shown as dotted lines above the sum. The multichain model fit yields higher persistence lengths and extension ratios than the single chain model fit for intermediate elastic responses.²⁸ As detailed in the caption of Figure 3, the intermediate responses have higher persistence lengths than those typically found.

The single chain and the multichain models are distinguishable by how well they fit multiple elastic responses to a single persistence or Kuhn length. For ease of discussion, we will consider only the persistence length. When multiple elastic responses are fit to a single chain model, the persistence lengths become very similar and can be fit quite well to a single persistence length for all of the elastic responses. In the example given in Figure 3b, a single persistence length of 4.4 Å gives a χ^2 of 1.96. The multichain, single persistence length fit (not shown) gives a 5.7 Å persistence length and a $2.54\chi^2$ as the characteristic parameters but fails to fit the intermediate responses. The persistence length of 4.4 Å for the single chain, single persistence length, corresponds to a diameter of 2.8 Å, further suggesting that even for multiple elastic responses in a single force plot a single chain is bridging the tip and the surface.

On the basis of the single chain model's success over the multichain model, and the small persistence lengths obtained from both the FJC and WLC corresponding to small diameters of chains, we conclude that the majority of our data represents the elastic stretching of a single polymer chain. It then follows that the polymer chain is left on the surface, or else multiple chain dynamics would be observed for the majority of the force plots. However, it seems reasonable that if the chain is extended to lengths comparable to the length of the entire chain, one might suspect that the chain remains on the tip. Indeed, we have observed in rare cases (5 of 700+) that entire force volumes (16×16 force plots) give rise to experimentally identical force plots over a lateral distance of a micrometer (data not shown). Each of these force plots exhibits the same elastic response, suggesting that there is indeed a single chain on the tip that is repeatedly stretched. This

(28) In both the single chain and multichain models the last elastic response is from one chain. This demands the same fitted values for the last response for both models. In Figure 3b (single chain model fit), the six elastic responses were fit by a single persistence length, resulting in a slightly different result for the last response than that for the multichain model used in Figure 3a.

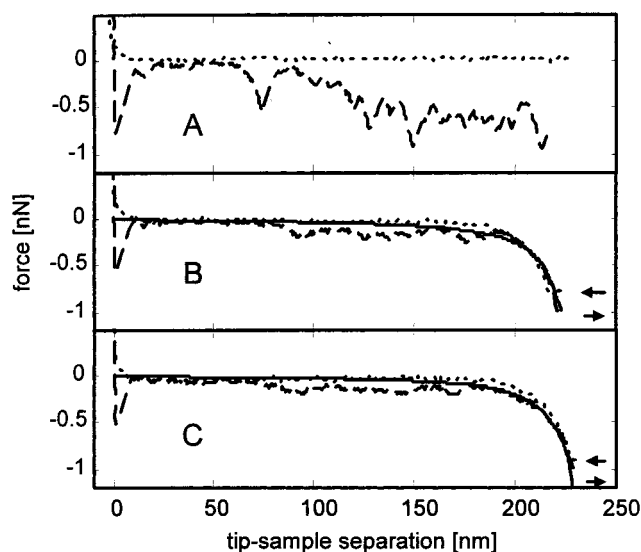


Figure 6. PS52400–P2VP28100 collected with a 100 nm trigger, 300 nm scan size, and at a scan rate of 1.95 Hz. All plots are sequential within the same force volume. There was 62.5 nm in lateral displacement between force plots. (A) Force–distance plot showing the tip approaching the surface (dotted) and subsequently pulling out an entangled group of two to four chains (dashed). (B) Here the advancing tip reversibly relaxes the chains before they have detached from the tip. The solid line is a fit to the elastic responses using the WLC model. The fit gave a 0.91 maximum extension ratio and 1.2 Å persistence length. (C) Subsequent force plot showing the same process as (B). WLC fit gave a 0.93 maximum extension ratio and 1.6 Å persistence length.

is not the case in most of the force plots and suggests that the removal of a chain from the surface is a rare event.

In studies on titin, Gaub and co-workers showed that the multiple elastic responses were due to separate domains unfolding in a single chain.¹⁰ Each domain unfolds under greater strain than the previous, showing that multiple attachments of the chain to the surface or tip were not significant in the elastic response. This is obviously not the case in Figure 3, as the third elastic response ruptures under the least strain. In our study, there are no rigid polymer domains along the length of the chain; consequently, we identify elastic responses which detach additional polymer from the surface/tip, allowing weaker attachments to be exposed and rupture at different forces.

We now discuss a case where we find that multiple chains give rise to the observed elastic response. Figure 6 depicts three consecutively collected force plots. In panel A the tip stretches the polymer and maintains that contact throughout the subsequent force plots, B and C, each collected at a different lateral position. The estimated contour length of the polymer between the tip and the surface is approximately 282 nm.²⁹ The molecular-weight-based length of the individual chains of PS52400–P2VP28100 are estimated to be 193 nm, well below the estimated length in Figure 6, suggesting that polymer chains are acting in series. The fitted values of the persistence length are 1.6 and 1.2 Å, using the WLC model. These values are well below the typical value of 3 Å. We have found that when the observed elastic response is the result of multiple chains in parallel, the fitted parameters have noticeable smaller characteristic lengths, i.e., per-

(29) The vertical tip sample separation is 230 nm. With 125 nm of lateral offset between the first and third plot the total tip sample separation is 262 nm. The maximum extension ratio is 0.93 giving an estimated contour length of 282 nm.

sistence lengths.³⁰ This is a result of the fact that the WLC model is intrinsically a single chain model. For the hypothetical case when there are two noninteracting chains in parallel, each with identical contour lengths between the tip and the surface, and thus the same extension ratios, the observed force would be twice as great as if there were one chain. Fitting this response by a single chain model would result in the characteristic length of one-half the true value, assuming the chains do not interact. For polymer ropes, where there are weak interactions between the chains in parallel, the extension ratios are consistent for all portions of chains contributing to the elastic response. This is a consequence of all the polymer chains having the same persistence length and the force acting on the polymer rope being uniformly distributed between the tip and the surface. When the polymer-polymer interactions do not introduce ordered structures, it is approximately correct that the average number of chains acting in parallel between the tip and the surface can be calculated by dividing the theoretical characteristic length by the fitted value of the characteristic length. The theoretical persistence length can be calculated by eq 6.³¹

$$q = l(1 - \cos \theta)^{-1} \quad (6)$$

Here l is the bond length (1.54 Å) and θ is the supplement to the bond angle (70.5), giving a theoretical persistence length for a C-C backbone of 2.31 Å. Thus our WLC model persistence length fits of 1.6 and 1.2 Å for the data in Figure 6b and Figure 6c indicate that the observed response is from a polymer rope, that is 1.5 to 2 chains wide, with a length that is 1.5 to 2 chains long, thus involving from 2 to 4 entangled polymer chains. It should be noted that of the approximately 200 000 force plots examined, these three are the only ones that demonstrate repeated stretching of polymer ropes attached to the surface.

There is no evidence of specific interactions between the tip and the chain; consequently we infer that the attachment of the polymer to the tip is through non-covalent bonds. The rupture force of such attachments is determined by the interfacial tension as well as the contact area, in principle allowing for the distinction between blocks of a block copolymer. In an attempt to distinguish the blocks that were studied here, we conducted contact angle measurements on P2VP films. Linear regression analysis of advancing contact angles of sodium chloride solutions yielded a critical surface tension of 65.8 ± 0.7 dyn/cm. The Zisman plot can be found in the Supporting Information. Pure water gave a contact angle of 55° , which through Young's equation gives an interfacial tension of 24.1 dyn/cm. Polystyrene has a surface energy of 33 dyn/cm³² and a contact angle of 88° ,¹⁶ giving an interfacial tension of 30.5 dyn/cm. Assuming that this similarity in interfacial tensions propagates to the interfacial tension of the polymer and the tip, detecting this difference is beyond the accuracy of our force measurement.³³ In the case of PS-P2VP the difference in interfacial tensions of

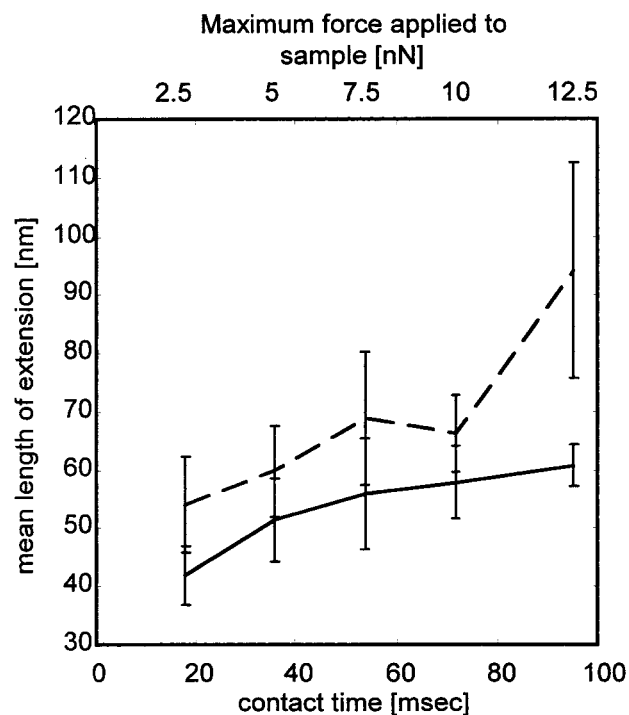


Figure 7. PS13800-P2VP47000 z scan speed 3300 nm/s. The lower solid line is the mean tip sample separation at the rupture of the elastic response. The upper dashed line is the estimated contour length of the chain based on the maximum extension ratios obtained from the WLC fits.

the two blocks with water is too small to detect. The use of block copolymers with significantly different interfacial tensions could help distinguish between polymer blocks, and possibly the mapping of surface segregation, as well as monitoring surface rearrangement as a function of solvent quality.

The contact time dependence of the elastic response was studied on PS13800-P2VP47000 (Figure 7). Contact time was increased by increasing the maximum applied pressure while maintaining a constant z scan speed of 3300 nm/s, and thus it is undetermined if the dependence is a function of contact time alone or if there is also an applied pressure component. Neither the rupture force of the elastic response nor the fitted values for the WLC and FJC model show a contact time dependence (Table 3, Supporting Information). However, we found a dramatic increase in the probability of an elastic response on increasing contact time (Table 3). It was also found that the relative probability of attaching a longer chain increases with contact time, as shown by the increase in average extension length of the elastic response (Figure 7). The upper line is the estimated contour length of the chain based on the maximum extension ratio from the WLC model. We conjecture that the increase in the average length of extension results from an improved attachment of the chain to the tip. There is no apparent contact time dependence on the rupture force of the elastic event, as shown in Table 3 (Supporting Information).

Conclusions

We have demonstrated the ability of AFM to elastically extend a single polymer chain from a surface into the overlying solvent. We have shown that the WLC and FJC models fit the nonlinear elastic response with equal success. Persistence lengths so obtained indicate the chains have ca. 2.5 Å diameters, comparable to the estimated monomer size. The extension ratio obtained

(30) Bemis, J.; Akhremitchev, B.; Al-Maawali, S.; Walker, G. Submitted for publication.

(31) Yamakawa, H. *Helical Wormlike Chains in Polymer Solutions*; Springer: New York, 1997; p 19.

(32) Israelachvili, J. *Intermolecular and Surface Forces*, 2nd ed.; Academic Press: San Diego, CA, 1992; p 204.

(33) The small amount of uncertainty in the sensitivity determination propagates to approximately 10% when using calibration standards of known force constants. As a result, there does not appear to be a trend in the rupture force of the elastic responses, as shown in Table 1.

from the fits, the length of the elastic response, and the estimated contour length of the chains demonstrate that we are extending the polymer chains approximately 35% of their entire chain length. We first noted an elastic response in a random block copolymer with fluorinated side chains.³⁴ We now show this phenomenon to also be present in both homopolymer and block copolymer systems. AFM may serve as a useful tool to stretch single polymer chains in many other polymeric systems. The low force of this elastic response may be the reason that it is often unnoticed, but as lower forces are probed, this phenomenon will need to be better understood.³⁵

(34) Akhremitchev, B. B.; Mohny, B. K.; Marra, K. G.; Chapman, T. M.; Walker, G. C. *Langmuir* **1998**, *14*, 3976–3982.

Acknowledgment. We acknowledge ONR for financial support (N0001-96-1-0735).

Supporting Information Available: Table of contact time dependence on elastic chain model fits, Zisman plot, Kuhn lengths with corresponding diameters, histograms of maximum extension ratios for both WLC and FJC models, histograms of length of extension and force of extension for each of the polymers studied. This material is available free of charge via the Internet at <http://pubs.acs.org>.

LA980853T

(35) **Note added in proof:** A related study published after acceptance of this paper is as follows: Ortiz, C.; Hadziioannou, G. *Macromolecules* **1999**, *32*, 780–787.